

The Stiffness of Statically Indeterminate Spindle Systems with Nonlinear Bearings

M. P. Soon and B. J. Stone

The Department of Mechanical and Materials Engineering, The University of Western Australia, Western Australia

The paper relates to the design of machine tool spindles for optimal static stiffness using computer simulation. Current trends are to have computer algorithms which are reliable and allow efficient and accurate programming. In particular, algorithms which may be repeatedly applied to model complex systems, by gradually building up to the final system, are extremely useful. The algorithms described allow the analysis of complex statically indeterminate spindles and provide stiffness values and deflected shapes. The algorithms may also be used with nonlinear bearing stiffnesses thus enabling the resulting nonlinear static stiffness of the spindle system to be predicted. The algorithms are also fast compared to normal methods and therefore allow the designer to investigate a range of design possibilities interactively.

Keywords: Design; Machine tools; Nonlinear; Spindles; Stiffness

1. Introduction

Perhaps the most common exercise in machine design is that of spindle specification. This involves taking into account the following design constraints:

Function.
Speed range.
Expected loads.
Accuracy.
Life.
Noise.

In turn, this requires the designer to specify or consider:

Shaft geometry.
Bearings: type, number, preload, lubrication, fit.

Alignment.

Thermal expansion.

Drive – type and position.

Stiffness and deflections.

Dynamic response and natural frequencies.

For machine tools it is generally accepted that the spindle is the most significant contributor to the static and dynamic stiffness of the machine tool. Ideally the designer aims to optimise both the static and dynamic stiffness of the spindle. It would, therefore, be very attractive to have an expert system that would accomplish this within certain specified constraints. The work described in this paper is a prerequisite of such an expert system.

For many years, a systems approach has been used for modelling the dynamic characteristics of structures [1] and was applied to machine tool spindles [2]. However, the equivalent approach for a static analysis, which could accommodate shear effects, multiple bearings (with radial and tilt stiffness) and multiple changes in shaft section, was not generally available as the problem was indeterminate. The objective of the work described in this paper was therefore to ensure that the systems approach used for the prediction of dynamic stiffness could also be used for static stiffness predictions. This enables a single set of data (defining the geometry, bearings, etc.) to be used for both the static and dynamic stiffness predictions.

As a result of the development of such an approach it has also been possible to investigate experimentally the effects of the nonlinear stiffness of bearings on optimum spindle stiffness (see [3, 4]). These nonlinear effects have been reported previously [5] but in the past were ignored in analysis. This paper describes the algorithms which were developed to allow the systems approach to be employed for static stiffness predictions. These algorithms are then used to investigate the effects of nonlinear bearing stiffness on the design of spindles for optimal static stiffness.

These algorithms, together with those for the analysis of dynamic stiffness, have since been incorporated into an expert system for optimising the static and dynamic stiffness of spindles [6].

Correspondence and offprint requests to: Professor B. J. Stone, Department of Mechanical and Materials Engineering, The University of Western Australia, Nedlands, Western Australia 6907. E-mail: bjs@mech.uwa.edu.au

2. Addition Algorithms

A spindle system may be considered to be made up of a series of shaft elements joined together axially with bearings added at discrete positions. Thus, it was decided to develop a method of static analysis which involved successively adding shaft elements or bearings, as desired, so that a complex spindle could be readily achieved. This had already been achieved for the dynamic analysis of spindles [2]. For the static analysis this required that routines be devised for determining the stiffness at one end of a shaft when it was added to an already existing spindle system. Consider such a shaft element.

2.1 Shaft Element

Consider first the case, as shown in Fig. 1, of an applied external force F at $x = L$ on the shaft element to be added as shown in Fig. 1. For static equilibrium this requires $-F$ at $x = 0$ and a moment $M = FL$ at $x = 0$, which are provided by reactions from the existing spindle to which it is attached. (Note moments are defined as positive anticlockwise.)

Now for small deflections,

$$\frac{\varphi_0}{F} = -\gamma_{L'L}L - \gamma_{L'L}$$

i.e. $\frac{dy}{dx} = \varphi + \gamma$

where φ is the slope from bending and γ is the slope from shear.

$$M = -EI \frac{d\varphi}{dx}$$

and

$$F = \lambda GA\gamma$$

If it is assumed that the radial and bending stiffness of the already existing spindle have been found experimentally, then, since the force and moment applied to the existing spindle are known, the deflection and slope at the join may be calculated. It follows that the objective of the analysis is to determine the deflection (y_L) and slope (φ_L) due to a force F at $x = L$ on the added shaft element, knowing the deflection (y_0) and slope (φ_0) at $x = 0$. If the same analysis is completed for an applied external moment M at $x = L$ on the shaft element to be added, then the radial and bending stiffness for the new spindle are

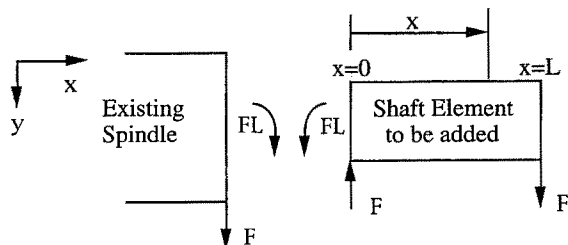


Fig. 1. Force and moment equilibrium of a shaft element with an applied external force.

known. Thus it is necessary to find y_L and φ_L knowing y_0 and φ_0 .

At section x ,

The shear force is,

$$F = \lambda GA\gamma \tag{1}$$

and the moment is $M = -F(L - x)$ so that

$$-F(L - x) = -EI \frac{d\varphi}{dx}$$

Integrating yields,

$$-F \left[Lx - \frac{x^2}{2} \right] + C_1 = -EI\varphi$$

when $x = 0$, $\varphi = \varphi_0$ so that $C_1 = -EI\varphi_0$ and thus

$$\varphi = \varphi_0 + \frac{F}{EI} \left[Lx - \frac{x^2}{2} \right] \tag{2}$$

Now the total slope is the sum of the slope due to bending plus the slope due to shear, thus

$$\frac{dy}{dx} = \varphi + \frac{F}{EI} \left[Lx - \frac{x^2}{2} \right] + \frac{F}{\lambda GA}$$

integrating,

$$y = \varphi_0 x + \frac{F}{EI} \left[\frac{Lx^2}{2} - \frac{x^3}{6} \right] + \frac{Fx}{\lambda GA} + C_2$$

when $x = 0$, $y = y_0$ so that $C_2 = y_0$ and therefore,

$$y = y_0 + \varphi_0 x + \frac{F}{EI} \left[\frac{Lx^2}{2} - \frac{x^3}{6} \right] + \frac{Fx}{\lambda GA} \tag{3}$$

Thus, if we introduce the concept of a static receptance we obtain,

$$\beta_{xL} = \frac{y_x}{F_{x=L}} = \frac{y_0}{F} + \frac{\varphi_0 x}{F} + \frac{1}{EI} \left[\frac{Lx^2}{2} - \frac{x^3}{6} \right] + \frac{x}{\lambda GA} \tag{4}$$

and

$$\beta'_{xL} = \frac{\varphi_x}{F_{x=L}} = \frac{\varphi_0}{F} + \frac{1}{EI} \left[Lx - \frac{x^2}{2} \right] \tag{5}$$

The notation adopted is the same as that presented by Bishop and Johnson [1] for dynamic receptances including damping, i.e. a prime (') indicates slope resulting from bending. If a similar analysis is conducted for an applied external moment M , we obtain,

$$\beta_{xL'} = \frac{y_x}{M_{x=L}} = \frac{y_0}{M} + \frac{\varphi_0 x}{M} - \frac{x^2}{2EI} \tag{6}$$

and

$$\beta'_{xL'} = \frac{\varphi_x}{M_{x=L}} = \frac{\varphi_0}{M} - \frac{x}{EI} \tag{7}$$

Using the static receptances derived above it is possible to build up a complex shaft using the same addition routine repetitively.

2.2 Series Addition of Shaft Elements

Consider the existing spindle to be system C with receptances γ . Then when an additional shaft (or system B) is added and an external force F is applied at $x=L_B$ on the additional shaft element we obtain, for static equilibrium, the state shown in Fig. 2.

From compatibility, y_{0_B} for system B equals y_{L_C} for system C and also φ_{0_B} for system B equals φ_{L_C} for system C .

Using linear superposition, y_{L_C} for system $C = \gamma_{LL}F + \gamma_{LL'}(-FL) = y_{0_B}$ for system B and hence for system B ,

$$\frac{y_{0_B}}{F} = \gamma_{LL} - \gamma_{LL'}L$$

Also the slope resulting from bending will be continuous (though the slope involving shear will not).

Using linear superposition, φ_{L_C} for system $C = \gamma_{L'L}(-FL) + \gamma_{L'L}F = \varphi_{0_B}$ for system B and hence for system B ,

$$\frac{\varphi_{0_B}}{F} = -\gamma_{L'L}L + \gamma_{L'L}$$

Thus substituting in Eqs (4) and (5) for y_{0_B}/F and φ_{0_B}/F ,

$$\beta_{xL} = \gamma_{LL} - \gamma_{LL'}L_B + [-\gamma_{L'L}L_B + \gamma_{L'L}]x + \frac{1}{EI} \left[\frac{Lx^2}{2} - \frac{x^3}{6} \right] + \frac{x}{\lambda GA} \quad (8)$$

and

$$\beta_{x'L} = -\gamma_{L'L}L_B + \gamma_{L'L} + \frac{1}{EI} \left[Lx - \frac{x^2}{2} \right] \quad (9)$$

When an external moment M is applied to the additional shaft element at $x=L_B$ we have the state shown in Fig. 3.

The opposite moment at $x=0_B$ on system B is required for static equilibrium. From compatibility, as above, y_{0_B} for system B equals y_{L_C} for system C and also φ_{0_B} for system B equals φ_{L_C} for system C .

Therefore, using linear superposition, y_{L_C} for system $C = \gamma_{LL}M = y_{0_B}$ for system B and hence for system B ,

$$\frac{y_{0_B}}{M} = \gamma_{LL'}$$

and φ_{L_C} for system $C = \gamma_{L'L}M = \varphi_{0_B}$ for system B and hence for system B ,

$$\frac{\varphi_{0_B}}{M} = \gamma_{L'L}$$

Thus, substituting in equations (6) and (7),

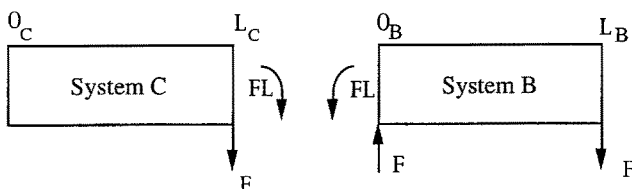


Fig. 2. Addition of a shaft element. (Applied external force at $x=L_B$ on system B .)

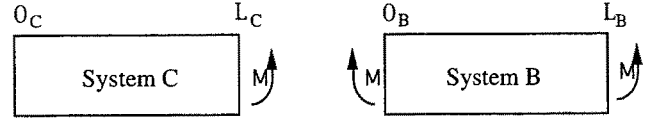


Fig. 3. Addition of a shaft element. (Applied external moment at $x=L_B$ on system B .)

$$\beta_{xL'} = \gamma_{LL'} + \gamma_{L'L}x - \frac{x^2}{2EI} \quad (10)$$

and

$$\beta_{x'L} = \gamma_{L'L} - \frac{x}{EI} \quad (11)$$

2.3 Addition of a Bearing

Consider the existing spindle to be a system C with receptances γ then when an additional bearing is added and an external force F applied to the shaft element we obtain the moments and forces on the system C and bearing as shown in Fig. 4.

If the radial and tilt bearing stiffnesses are assumed to be known, considered to be linear at this stage, and defined as,

k = radial stiffness

k' = tilt stiffness

for the two representations in Fig. 4 to be identical,

$$F = F_1 + F_2 \quad (12)$$

the deflection y_{L_C} will be the same on the bearing and on the shaft, i.e. system C . Using linear superposition,

$$y_{L_C} = \gamma_{LL}F_1 + \gamma_{LL'}M_1 = \frac{F_2}{k} \quad (13)$$

and the total slope will be the same on the bearing and on the shaft, i.e. system C . Thus

$$\varphi_{L_C} + \frac{F_1}{\lambda GA} = \gamma_{L'L}F_1 + \gamma_{L'L}M_1 + \frac{F_1}{\lambda GA} = \frac{M_1}{k'} \quad (14)$$

We require for the new system A (i.e. system B plus the additional bearing),

$$\alpha_{LL} = \frac{y_{L_C}}{F}, \quad \alpha_{L'L} = \frac{\varphi_{L_C}}{F}$$

Thus eliminating F_2 from (12) and (13)

$$\gamma_{LL}F_1 + \gamma_{LL'}M_1 = \frac{(F - F_1)}{k}$$

rearranging,

$$F_1 \left(\gamma_{LL} + \frac{1}{k} \right) + \gamma_{LL'}M_1 = \frac{F}{k} \quad (15)$$

Now rearranging (14)

$$F_1 = M_1 \frac{\left(\frac{1}{k'} - \gamma_{L'L} \right)}{\left(\gamma_{L'L} + \frac{1}{\lambda GA} \right)} \quad (16)$$

and substitute for F_1 in (15)

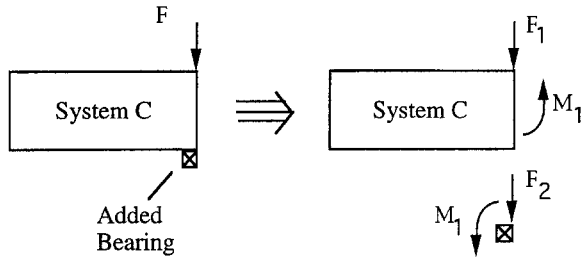


Fig. 4. Addition of a bearing. (Applied external force at $x=L_C$ on system C.)

$$M_1 \left[\frac{\left(\frac{1}{k'} - \gamma_{L'L'}\right)\left(\gamma_{LL} + \frac{1}{k}\right)}{\left(\gamma_{L'L} + \frac{1}{\lambda GA}\right)} + \gamma_{LL'} \right] = \frac{F}{k}$$

therefore,

$$M_1 = \frac{F}{k} \frac{\left(\gamma_{LL} + \frac{1}{\lambda GA}\right)}{\left[\left(\gamma_{LL} + \frac{1}{k}\right)\left(\frac{1}{k'} - \gamma_{L'L'}\right) + \gamma_{LL'}\left(\gamma_{L'L} + \frac{1}{\lambda GA}\right)\right]} \quad (17)$$

From (13) $y_{L_C} = \gamma_{LL}F_1 + \gamma_{LL'}M_1$ and substituting for F_1 from (16)

$$y_{L_C} = \left[\frac{\gamma_{LL}\left(\frac{1}{k'} - \gamma_{L'L'}\right)}{\left(\gamma_{L'L} + \frac{1}{\lambda GA}\right)} + \gamma_{LL'} \right] M_1$$

We require $\alpha_{LL} = y_{L_C}/F$ which from the above and substituting for M_1 from (17) after some manipulation yields,

$$\alpha_{LL} = \frac{1}{k} \frac{\gamma_{LL}\left(\frac{1}{k'} - \gamma_{L'L'}\right) + \gamma_{LL'}\left(\gamma_{L'L} + \frac{1}{\lambda GA}\right)}{\left[\left(\gamma_{LL} + \frac{1}{k}\right)\left(\frac{1}{k'} - \gamma_{L'L'}\right) + \gamma_{LL'}\left(\gamma_{L'L} + \frac{1}{\lambda GA}\right)\right]} \quad (18)$$

We also require $\alpha_{L'L} = \phi_{L_C}/F$. From (14) $\phi_{L_C} = \gamma_{L'L}F_1 + \gamma_{L'L'}M_1$ and substituting for F_1 from (16) and M_1 from (17) and rearranging gives,

$$\alpha_{L'L} = \frac{1}{k} \frac{\gamma_{L'L}\left(\frac{1}{k'} - \gamma_{L'L'}\right) + \gamma_{L'L'}\left(\gamma_{L'L} + \frac{1}{\lambda GA}\right)}{\left[\left(\gamma_{LL} + \frac{1}{k}\right)\left(\frac{1}{k'} - \gamma_{L'L'}\right) + \gamma_{LL'}\left(\gamma_{L'L} + \frac{1}{\lambda GA}\right)\right]} \quad (19)$$

To complete the set of static receptances when a bearing is added it is necessary to also consider an external moment M applied on the shaft element we obtain the moments and forces on the spindle and bearing as shown in Fig. 5.

For the two representations to be identical,

$$M = M_1 + M_2$$

and using a similar approach to that used for an external force, the following relationships are obtained.

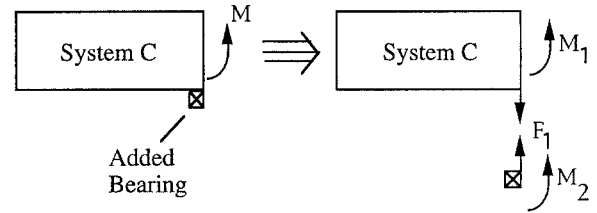


Fig. 5. Addition of a bearing. (Applied external moment at $x=L_C$ on system C.)

$$\alpha_{LL'} \quad (20)$$

$$= \frac{1}{kk'} \frac{\gamma_{LL'}}{\left[\left(\gamma_{LL} + \frac{1}{k}\right)\left(\frac{1}{k'} - \gamma_{L'L'}\right) + \gamma_{LL'}\left(\gamma_{L'L} + \frac{1}{\lambda GA}\right)\right]}$$

$$\alpha_{L'L'} \quad (21)$$

$$= \frac{1}{k'} \frac{\gamma_{L'L'}\left(\gamma_{LL} + \frac{1}{k}\right) + \gamma_{L'L}\gamma_{LL'}}{\left[\left(\gamma_{LL} + \frac{1}{k}\right)\left(\frac{1}{k'} - \gamma_{L'L'}\right) + \gamma_{LL'}\left(\gamma_{L'L} + \frac{1}{\lambda GA}\right)\right]}$$

With the static receptances derived above it is possible to systematically build a spindle system and determine its static stiffness. Thus, consider a typical spindle and its division into constituent elements, as shown in Fig. 6.

As the force is applied at the righthand end, the spindle is built from the left. The first shaft element {1} is a free/free shaft and therefore has no static stiffness. We thus start with the bearing {2} and its static receptances are given by,

$$\gamma_{LL} = \frac{1}{k}, \quad \gamma_{L'L'} = \frac{1}{k'} \quad \text{and} \quad \gamma_{L'L} = \gamma_{LL'} = 0$$

This assumes no coupling between the radial and tilt stiffnesses.

These receptances define the current system C. The shaft element {3} is then added as system B using Eqs (8) to (11) with $x=L_3$, the length of the element. This produces β_{LL} , $\beta_{L'L}$, $\beta_{LL'}$ and $\beta_{L'L'}$ for the sum of the first three elements. We now define the sum of the first three elements as the current spindle, i.e. system C. Thus, β_{LL} , $\beta_{L'L}$, $\beta_{LL'}$ and $\beta_{L'L'}$ become γ_{LL} , $\gamma_{L'L}$, $\gamma_{LL'}$ and $\gamma_{L'L'}$ for the addition of the shaft element 4 which is then the current system B. The procedure is then the same as for the addition of element {3} and we find γ_{LL} , $\gamma_{L'L}$, $\gamma_{LL'}$ and $\gamma_{L'L'}$ for the first four elements.

The bearing {5} is then added using Eqs (18) to (21) and produces α_{LL} , $\alpha_{L'L}$, $\alpha_{LL'}$ and $\alpha_{L'L'}$ for the sum of the first five elements and these become γ_{LL} , $\gamma_{L'L}$, $\gamma_{LL'}$ and $\gamma_{L'L'}$ of the new current system C for the addition of the shaft element {6} in the same manner as the previous shaft elements. The final values are those for the whole spindle and the static stiffness at the point of application of the force is $1/\gamma_{LL}$.

The deflected shape is obtained by working back through the elements and determining the interface forces and couples. This allows the deflection and slope at bearing {2} to be calculated. The shaft element {1} has no bending within it so the deflection is simply the extrapolation of the slope of bearing {2}. Then for other shaft elements in turn each have a known deflection and slope at $x=0$ and from Eqs (4) to (7) the deflection along the element may be obtained. The deflection

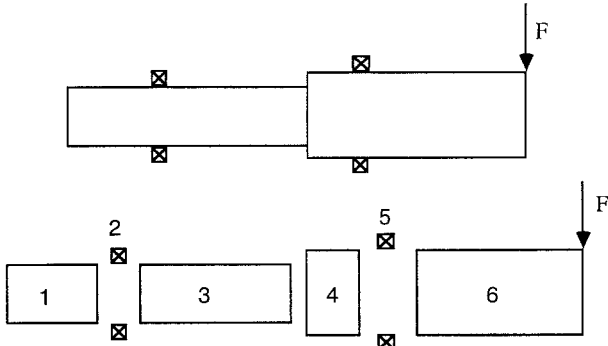


Fig. 6. Division of spindle into elements.

and slope at $x = L$ for each shaft element becomes the deflection and slope for the next shaft element at $x = 0$, and so on.

For a force or moment applied at other than the end of a spindle the same approach may be easily adapted. Consider the spindle shown in Fig. 7 with the load applied in the position shown. It is easy to consider this as two spindles joined together but with each spindle having a force and moment applied at an end as shown in Fig. 8.

To determine the force and moment on each spindle it is necessary to ensure that the deflection and slope due to bending are the same at the join. To use the equations previously developed we must build each spindle from the left so the Spindle *R* is rotated horizontally as shown in Fig. 9. Note the associated sign change on the moment. Also, the slope at the end will now have to be negative to ensure the same slope as for spindle *L*. Thus,

$$y_L = [\gamma_{LL}]_L (F - F_R) - [\gamma_{LL}]_L M_R = [\gamma_{LL}]_R F_R - [\gamma_{LL}]_R M_R$$

and

$$\phi_L = [\gamma_{L'L}]_L (F - F_R) - [\gamma_{L'L}]_L M_R = -[\gamma_{L'L}]_R F_R - [\gamma_{L'L}]_R M_R$$

where for example $[\gamma_{L'L}]_L$ is a receptance of the complete spindle *L*.

From these equations it is possible to solve for F_R and M_R in terms of F and then the stiffness y_L/F may be obtained. The deflected shape may then be found by treating each spindle separately with the relevant force and moment applied.

A typical output from a computer program written to include these algorithms is shown in Fig. 10. The stiffness shown applies to the point of application of the force. The deflected shape is shown without units as the force magnitude was not specified. However, if the force is specified then a dimensioned deflected shape is given. It should be noted that the computer code is quite simple and efficient because the same addition algorithms are applied repeatedly. The program has no difficulty with the fact that with tilt stiffnesses in the bearings

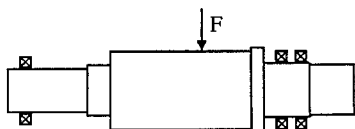


Fig. 7. Spindle with load applied away from an end.

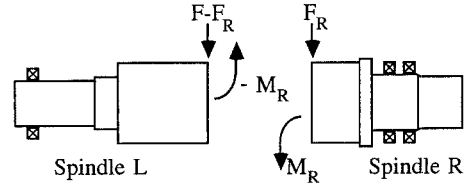


Fig. 8. Forces and moments on two spindles, *L* and *R*.

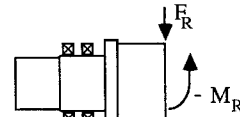


Fig. 9. Spindle *R* rotated horizontally.

the system is indeterminate even before the third bearing is added.

3. Nonlinear Bearings

It is known that bearings exhibit nonlinearity [5], but this has largely been ignored in the past owing to the difficulty of modelling this effect. It is possible to include the nonlinearity of the bearings in the modelling of the static stiffness of spindle systems using the systems approach method.

Lacey et al. [5] developed the variload spindle (a hydraulically actuated variable preload bearing unit, no longer available) to allow bearing preload to be varied with running speed. Their work involved the measurement of the static stiffness of angular rolling element bearings under different preloads. Figure 11 shows the radial load deflection characteristics as published by Lacey [5] for a 7024 angular contact bearing under low, medium and high preloads.

These curves clearly show the nonlinear characteristics of the bearing and that the nonlinearity can be seen to closely follow a cubic curve under low and medium preloads. However, under high preload condition, the nonlinearity follows a quadratic curve.

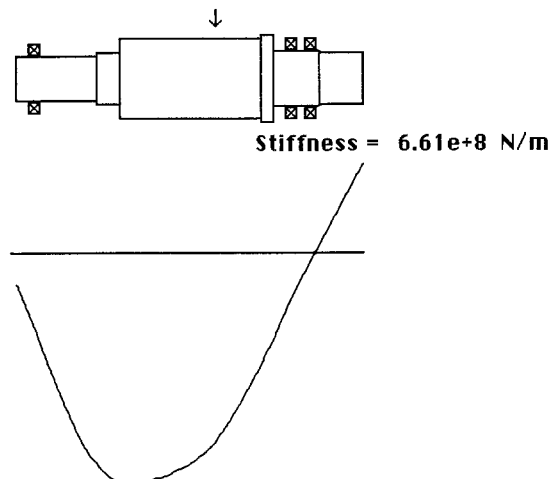


Fig. 10. Typical output from program.

It follows that if the equation representing the required nonlinear load-deflection relationship of the bearing can be determined, then the nonlinearity of the bearing under consideration can be modelled. The nonlinear load-deflection characteristic of the bearing under medium and high preload conditions was therefore modelled using a cubic equation of the form,

$$y = ax^3 + bx^2 + cx + d$$

To obtain the exact cubic equation which can represent the nonlinear relationship between the applied radial load P and the bearing radial deflection u for medium preload bearings, load deflection values were taken from Lacey's medium preload curve (Fig. 11) and a cubic equation as shown below was derived.

$$P = 7.65 \times 10^{16} u^3 - 8.58 \times 10^{12} u^2 + 4.41 \times 10^8 u \quad (22)$$

where u is in metres and P is in Newtons.

A nonlinear load-deflection curve derived using Eq. (22) can be seen in Fig. 12 and is found to be in close agreement with Lacey's curve (Fig. 11).

Since the stiffness of the bearing can be represented by the slope of the load-deflection curve, differentiating Eq. (22) gives the nonlinear radial stiffness equation for the medium preload bearing at a deflection u , i.e.

$$k_r = \frac{dP}{du} = 22.95 \times 10^{16} u^2 - 17.16 \times 10^{12} u + 4.41 \times 10^8 \quad (23)$$

and the flexural or tilt stiffness of the bearing was taken to be,

$$k_t = \frac{k_r}{10^4} \quad (24)$$

4. The Nonlinear Stiffness of Spindle Systems

The nonlinear static stiffness of a spindle system can therefore be modelled using the nonlinear bearing static stiffness equa-

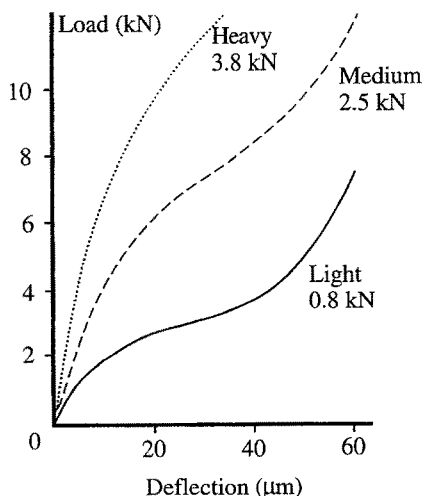


Fig. 11. Load-deflection curves for a bearing with different preloads. (After Lacey [5]).

tions by initially setting the bearing stiffness k_r to 4.41×10^8 N/m, (i.e. from Eq. (23), when $u=0$) and $k_t = 4.41 \times 10^4$ N/m from Eq. (24)).

Using the previously derived receptance equations, the receptance and hence the deflection at the spindle nose subjected to an applied load of say 50 N can be determined for a spindle system with dimensions as shown in Fig. 13. The resulting deflection and load values enable a point on the nonlinear spindle load-deflection curve to be plotted.

To obtain the next point on the nonlinear spindle load-deflection curve, i.e. adding an extra 50 N load, it is first necessary to find the new (i.e. under the current loads) values of k_r and k_t for each bearing. This can be achieved by finding the loads acting on the bearings by working backwards as described previously for the original 50 N load applied at the spindle nose. The deflection at each bearing can then be found knowing the force and the stiffness, and hence the new values of k_r and k_t may be obtained for each bearing using Eqs (23) and (24). The extra spindle deflection caused by the extra applied load of 50 N with the new bearing stiffnesses can then be calculated and added to the previous spindle deflection caused by the first 50 N load. This total spindle deflection is then plotted against the total applied load on the spindle, which is now 100 N, thus giving the second point on the nonlinear spindle load-deflection curve. The above process is repeated with load increments of 50 N until a load required, say 1.2×10^4 N, has been reached.

The predicted nonlinear load-deflection characteristics for a typical spindle system with dimensions as shown in Fig. 13 for three different bearing spans can be seen in Fig. 14. To check for accuracy, load increments smaller than 50 N were tried and found to have no effect on the accuracy of the spindle load-deflection curve. A further check was made by applying a full load on the same spindle system with zero load-bearing characteristics. The load on each bearing was then determined and from the nonlinear bearing stiffness plot, the effective linear stiffness of each bearing was determined and

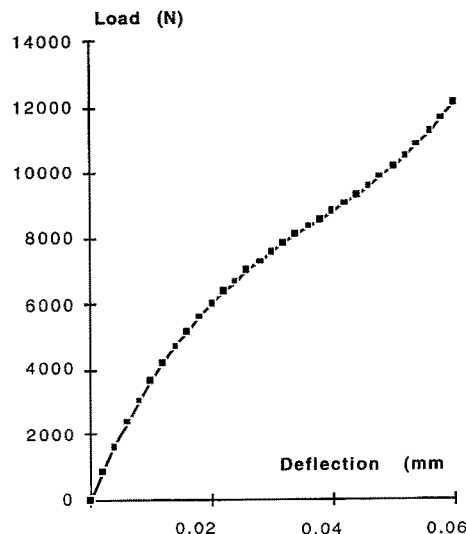


Fig. 12. Predicted load-deflection curve for bearing with medium preload.

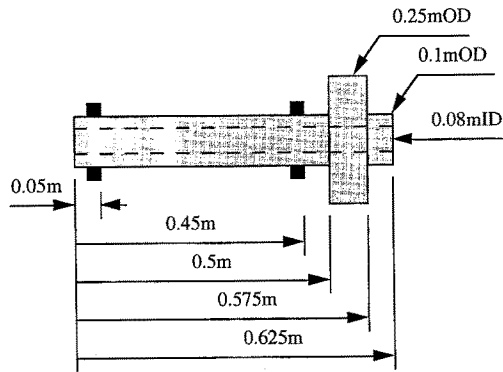


Fig. 13. Spindle dimensions. Young's modulus of elasticity $E = 2 \times 10^{11} \text{ N/m}^2$ and the shear modulus $G = 8 \times 10^{10} \text{ N/m}^2$.

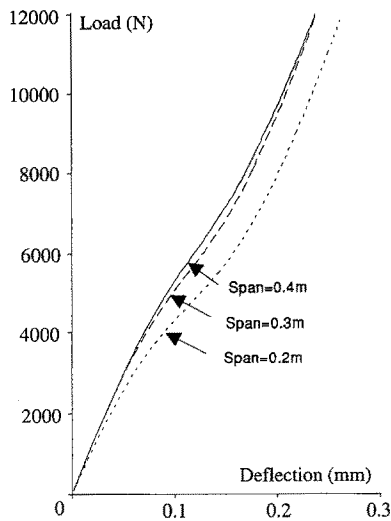


Fig. 14. Predicted nonlinear stiffnesses of the spindle system for three different bearing spans.

used for the next iteration. It was found that after two iterations, the same result as before was achieved.

5. The Effect of Nonlinear Bearings on Optimal Design of Spindle Systems

The effect of the nonlinearity of the bearing on the deflection and stiffness of a typical spindle system with parameters as shown in Fig. 13 can be seen in Figs 15 and 16. Note that the stiffness of the spindle system decreases as the applied load increases and is most sensitive at the lower range of the applied loads, i.e. as the applied load increases from zero, the stiffness decreases rapidly until a point is reached where the decrease is less severe, i.e. from 6 kN upwards. Note that if linear bearings were assumed, the spindle static stiffness would be constant for all applied loads.

Also, the nonlinear effect of the bearing has resulted in slightly different optimum spans for different applied loads. The optimum spans range from 0.35 to 0.4 m, depending on

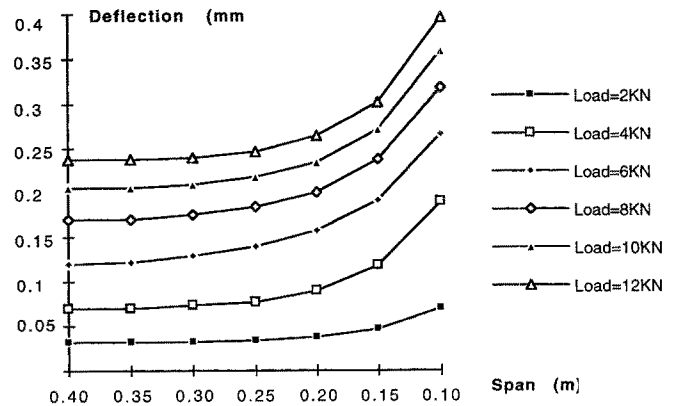


Fig. 15. The effect of nonlinear bearings on the spindle nose deflection.

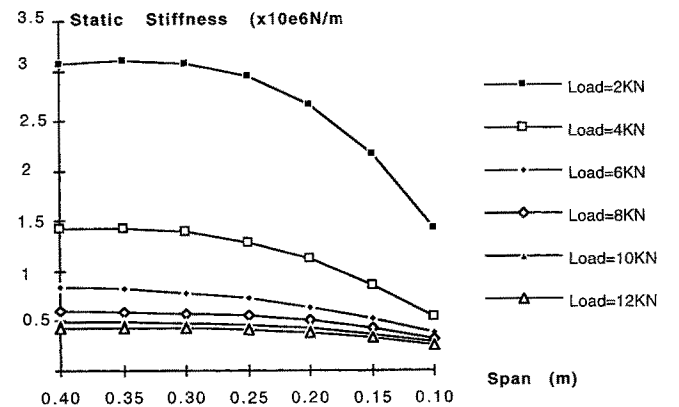


Fig. 16. The effect of nonlinear bearings on the spindle nose stiffness.

the magnitude of the applied load. Note that a correctly chosen bearing span is more critical at lower applied loads, as, under these lower loads, the spindle static stiffness decreases rapidly when the span is decreased (Fig. 16). Again if the nonlinearity of the bearing stiffness was ignored, the optimum span would be the same for all values of applied loads.

From the above predictions, it can be seen that the stiffness of spindle systems varies with the magnitude of the applied force. Therefore, for optimum design, it would be helpful if the nonlinear effect of bearings can be included in the prediction of the static stiffness of spindle systems.

6. Conclusions

The systems approach described above, together with the concept of static receptances, allows very rapid calculation of stiffness and deflection for complicated spindles with multiple bearings exhibiting nonlinear and both radial and tilt stiffness. These spindles are statically indeterminate and hence the approach has many advantages. Comparisons with far more complex computer programs show excellent agreement. It is thus possible to perform parameter optimisation in a very short

time and this is proving to be very attractive to designers who need to be able to operate interactively.

The algorithms described in this paper together with those for the analysis of dynamic stiffness have been successfully incorporated into an expert system for optimising the static and dynamic stiffness of spindles [6].

References

1. R. E. D. Bishop and D. C. Johnson, *The Mechanics of Vibration*, Cambridge University Press, London, 1960.
2. S. J. Potter and B. J. Stone, "The calculation of the response of spindle-bearing systems to oscillating forces", MTIRA Research Report 55, 1974.
3. R. J. Lambert, A. Pollard and B. J. Stone, "Some characteristics of rolling element bearings under oscillating conditions", MTIRA Report VI, December 1981.
4. B. J. Stone, "The state of the art in the measurement of the stiffness and damping of rolling element bearings", Keynote Paper, *Annals CIRP*, 31(2), 1982.
5. S. J. Lacey, F. P. Wardle and S. Y. Poon, "A high speed bearing arrangement for CNC machine tool spindles", RHP Bearings 1981.
6. M. P. Soon and B. J. Stone, "A knowledge-based system for the design of machine tool spindles", *International Journal of Advanced Manufacturing Technology* (submitted).

Nomenclature

A	area of cross-section
E	Young's modulus
F	applied force
G	shear modulus
I	second moment of area
L	length of shaft element
M	bending moment
y	horizontal direction perpendicular to X,Z -plane
x	position along shaft
γ	slope resulting from shear
λ	shear factor for section
φ	slope resulting from bending

Parameters with subscripts

α	static receptance after addition of bearing
β	static receptance after addition of shaft element
γ	static receptance of existing shaft system

Subscripts: The static receptances have two subscripts which indicate, first, the position of the displacement or slope and secondly the position of the applied force or moment. Slope and moment are differentiated from deflection and force by the addition of a prime, e.g. L' represents the slope or moment at the position L .